

POÁS VOLCANO, COSTA RICA: GEOLOGY OF THE SUMMIT REGION AND SPATIAL AND TEMPORAL VARIATIONS AMONG THE MOST RECENT LAVAS

JEROME T. PROSSER^{1,*} and MICHAEL J. CARR²

¹*Department of Earth Sciences, Dartmouth College, Hanover, NH 03755, U.S.A.*

²*Department of Geological Sciences, Rutgers University, New Brunswick, NJ 08903, U.S.A.*

(Received November 25, 1986)

Abstract

Prosser, J.T. and Carr, M.J., 1987. Poás volcano, Costa Rica: Geology of the summit region and spatial and temporal variations among the most recent lavas. In: S.N. Williams and M.J. Carr (Editors), Richard E. Stoiber 75th Birthday Volume. *J. Volcanol. Geotherm. Res.*, 33: 131-146.

The recent eruptive history of Poás volcano is described here on the basis of field mapping of the summit area. This period, which may represent 10 to 20,000 years and less than 10% of the history of the volcano, began with caldera formation. Subsequent events included: composite cone construction, faulting and flank subsidence, flank fissure eruption, and multiple crater collapses. Local and regional structures have controlled the locations of summit vents and flank cinder cones.

Chemical compositions of lavas of known stratigraphic position demonstrate temporal magmatic variation at Poás. Three similar felsic to mafic magmatic sequences occurred at the summit. The first and second sequences were separated by flank and summit eruptions of a distinct magma batch, enriched in TiO_2 and P_2O_5 . The three felsic to mafic sequences appear to be cyclical, and the repeated, similar variations are interpreted as progressive tapping of zoned magma bodies developed repeatedly from a common parent by similar crystal fractionation processes. The breaks between the three sequences correlate with shifts or major modifications of the eruptive center. The chemical composition of the most recent lava, erupted in 1954, indicates that the volcano is near the end of the present sequence.

The lavas are calc-alkaline basalts and andesites that are similar to the mafic lavas that comprise the bulk of the Central American volcanic front. The samples can be divided into 3 spatial-temporal-geochemical groups. A summit group that represents the most recent activity; a TiO_2 -rich group that erupted primarily on the south flank about 7500 yr. B.P.; and an Al_2O_3 -rich group that erupted primarily from vents north of the presently active Main Crater. Geochemical variations and projections into pseudoternary CMAS diagrams suggest a moderate pressure for the summit group, that is, a magma chamber at intracrustal to subcrustal depths. The Al_2O_3 -rich group define smaller primary phase volumes for olivine and plagioclase, which suggests a deeper and/or more water-rich magma chamber. The TiO_2 -rich group appears to be a batch of mixed magma with the summit group magma as one endmember and a less siliceous magma as the other.

Introduction

Poás Volcano is a structurally complex stra-

tovolcano, one of 41 historically active volcanoes in the Central American volcanic chain which extends 1100 km from Guatemala to Costa Rica. Volcanism in this chain is associated with subduction of the Cocos Plate north-

*Present address: Texasgulf Minerals and Metals, P.O. Box 3810, Chapel Hill, NC 27515, U.S.A.

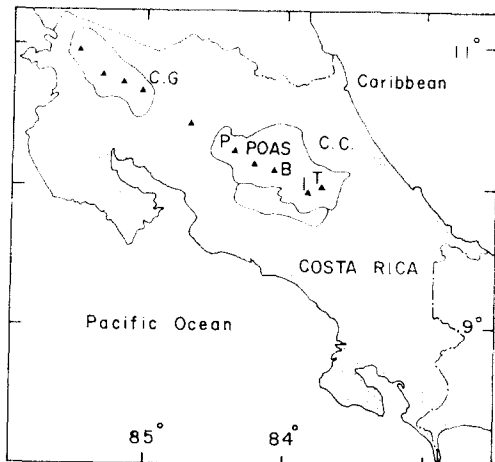


Fig. 1. Location map. C.C. is Cordillera Central, C.G. is Cordillera de Guanacaste, P is Platanar volcano, B is Barba, I is Irazú, T is Turrialba. The Meseta Central is the unlabelled region adjacent to the Cordillera Central.

eastward beneath the Caribbean Plate (Molnar and Sykes, 1969).

Poás and the adjacent volcanic centers, Platanar-Porvenir, Barba and Irazú-Turrialba, form a large massif of overlapping flows and pyroclastic deposits (Fig. 1). This massif, the Cordillera Central, is flanked on the trenchward side by a structural depression, the Meseta Central, in which volcanic deposits erupted from the Cordillera Central are well exposed in deep river cuts (Williams, 1952). Faults bounding the Meseta Central strike parallel to the volcanic front, about N60W.

Poás volcano rises 1300 m above its base at 1400 m and encompasses a volume of about 100 km³. Relative to other Central American volcanoes, Poás and the other volcanoes of the Cordillera Central are more massive and have higher summit elevations. In part, the high summit elevations of the Cordillera Central are due to their position overlying a massive volcanic pile of welded and non-welded ignimbrites and lava flows (Williams, 1952). Poás is less than 1.0 m.y. old because Sáenz (1982) has reported a radiometric age of 0.98 m.y. for an ignimbrite that crops out at the base of Poás. Allegre and Condomines (1976) used U and Th isotope ratios to infer that the magma source

for Irazú formed about 100,000 yr. B.P. and that of Poás formed about 50,000 yr. B.P.

Poás has a rounded dome-like shape, probably caused by repeated decapitation of the volcano during caldera-forming events. The flanks of the volcano slope gently in all directions except to the north, where higher rainfall has caused deeper erosion. The southern and western flanks are heavily populated and used for sugar cane, coffee, and dairy farms. A national park occupies the summit, which is easily reached via a paved road. Unlike the summit, the flanks have poor exposure and will require further study in order to completely describe the geology at Poás.

The stratigraphic data on the summit of Poás, summarized here, are based on the detailed geologic map of Prosser (1983). These data will be useful for future assessments of the volcanic hazards because knowledge of a volcano's geologic history is an essential requirement for estimating the nature of future eruptions. Furthermore, the sequence of 14 reasonably fresh lava and scoria samples provides another example of temporal variation in magma chemistry. In the case of Poás, this sequence represents a brief span late in the history of a large complex composite cone. The supplementary samples, collected from the flanks of Poás and from several parasitic cones, demonstrate that there is no single, simple magma body feeding the entire complex.

Data

Historic activity

During historic time Poás has been in a state of nearly continuous mild activity, which consists primarily of fumarolic emissions and occasional geyser-like phreatic eruptions, generally through a shallow crater lake (Vargas, 1979; Simkin et al., 1981; Casertano et al., 1983). In addition, powerful vulcanian blasts, milder strombolian explosions and a small lava flow have occurred. The most powerful historic

eruption at Poás occurred in 1910 when a vulcanian or phreatomagmatic eruption cloud reached 8 km in height and caused ashfall in San Jose 33 km to the southwest (Vargas, 1979). A moderate sized eruption during 1953–1955 featured all types of activity. The result of this eruption was the creation of a 25 meter high intra-crater cone, a small lava flow in 1954, and then a pit crater, into which one third of the intra-crater cone and most of the lava flow collapsed (Krushensky and Escalante, 1967). Laguna Caliente, a hot, acid lake (40–60°C, pH=0.1), presently occupies the pit crater, although it has been vaporized or ejected during periods of moderate activity.

A unique feature of some eruptions at Poás is the occurrence of pyroclastic sulfur. The pyroclastic sulfur particles and their origin are discussed in Francis et al. (1980) and Bennett and Raccichini (1978). Non-eruptive activity at Poás consists of degassing from fumaroles on the east and north sides of the intra-crater cone. Since 1981 fumarole temperatures have sometimes exceeded 700°C and SO₂ output was, at most, about 600 tons/day (R.E. Stoiber, pers. commun., 1983). Incandescence due to heating of the existing cone rocks can be seen in many of the fumarolic vents. Poás last erupted December 26, 1980.

Rymer and Brown (1984) report periodic changes in gravity at the summit of Poás during April–May, 1983. The volcano was in a fumarolic state of activity and the gravity field varied with a period of about 30 days and an amplitude of about 0.1 mgal. The variation was attributed to either small movements in a shallow subsurface magma body or changes in the extent of vesiculation of the magma.

Major structures

Volcanic structures and features found on the flanks and summit of Poás indicate that the volcano has had a long and complex eruptive history. The largest of these volcanic features are two calderas, one nested within the other

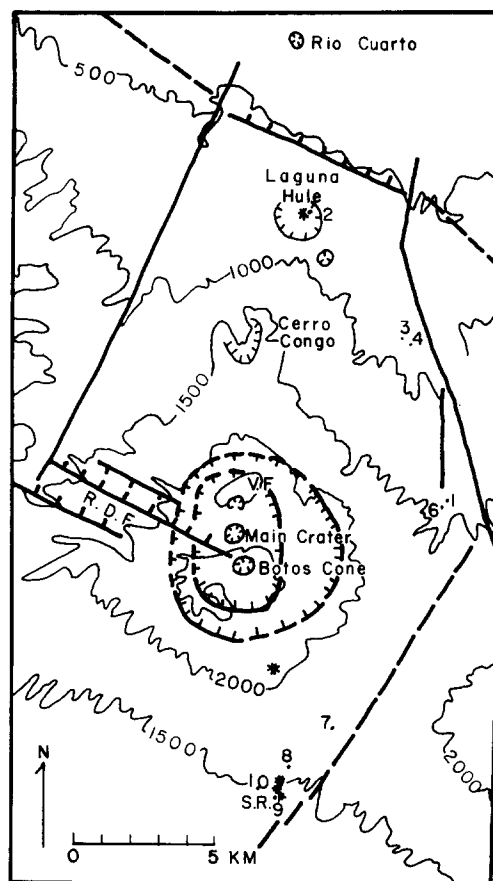


Fig. 2. Major structures of Poás. V.F. is Von Frantzius Cone. S.R. is Sabana Redonda. R.D.F. is Rio Desague fault. Asterisks are small cones. Numbers are locations of samples P01–P010. Bold lines are faults.

(Fig. 2). These structures are not well preserved and were identified by topographic breaks in the slopes of the volcano (Thorpe et al., 1981). The larger of the two calderas is about 6 km in diameter. The inner caldera is elliptical with a N–S major axis of 4 km. These calderas have been filled in by later eruptions and have served as physical barriers between summit volcanism and deposition on the flanks.

Several large volcanic structures have developed since formation of the last caldera. The largest and oldest of these is the Von Frantzius Cone, a highly eroded composite cone with a south-facing breached crater. Two km south of Von Frantzius is a smaller, younger composite cone called Botos Cone. Situated between the

two composite cones is the Main Crater of Poás, the site of all historic activity. The outer rim of the Main Crater is 0.8 km in diameter and encloses two smaller, nested craters. All are collapse craters, including a small pit crater, which is the site of the hot, acid lake.

The western flank of Poás is dominated by a graben extending from Botos Cone to the western base of the volcano. The axis of the graben strikes N60W, parallel to the volcanic front and the larger tectonic-structural depression south of Poás, the Meseta Central. Subsidence of the west flank probably occurred along re-activated tectonic faults originally associated with formation of the Meseta Central. The graben is bounded on the south by the Rio Desague fault scarp (Fig. 2) which has 400 m relief, and on the north by a series of smaller step faults.

On the southern flank, near the town of Sabana Redonda, is a line of cinder cones oriented north-south. These cones are relatively recent and may have been active simultaneously with late stages of eruption from Botos Cone (see discussion below). North of Poás are several vents that together with Poás form a well-defined N-S lineation (Fig. 2). At the base of the northern flank is Cerro Congo, a parasitic, composite cone. Three km north of Cerro Congo is Laguna Hule caldera, which is 2 km in diameter and contains a lake as well as an intracaldera cone. Six km further north is Laguna Rio Cuarto, a maar.

Stoiber and Carr (1973) noted N-S alignments of volcanic features throughout the Central American volcanic belt. They proposed that the N-S alignments represented the axis of maximum horizontal compression in the volcanic belt. Nakamura (1977) found that volcanic vents at polygenetic volcanoes such as Poás are commonly aligned parallel to the direction of maximum horizontal compression generated along the associated subduction zone. However, in Central America, the axis of maximum horizontal compression in the subduction zone, as defined by focal mechanisms (Molnar and Sykes, 1969), is N30E and not

N-S. The reason for the discrepancy between the stress field in the subduction zone and the stress field in the volcanic belt is not clear.

Intersections of structures appear to control vent locations (Fig. 2). Von Frantzius Cone is located at the intersection of the N-S lineament and the extension of the inner caldera. Botos Cone and the Main Crater are located where the two main faults bounding the small west flank graben intersect the N-S lineament.

Stratigraphy and structure of the summit

A thick lapilli tuff sequence that radiocarbon measurements indicate is more than 40,000 years old (U.S.G.S. Sample #W5232; Prosser, 1983) covers the flanks of Poás. This deposit, referred to here as the Lapilli Tuff, is overlain on the flanks by only a thin veneer of later air-fall deposits. The Lapilli Tuff appears to be the product of the later of the two caldera-forming eruptions. The thinness of the overlying airfall section indicates that the caldera walls and the low explosivity of the eruptions restricted deposition of most later volcanic products to the summit region. The stratigraphy exposed in the summit region, therefore, begins with this Lapilli Tuff.

Lava flows and airfall tephra are exposed in the Rio Desague fault scarp and in the walls of the Main Crater. These exposures represent a reasonably complete record of volcanic activity at Poás for a period covering at least the last ten thousand years. Although lava flows are normally well preserved, tephra are generally very poorly preserved, often having been weathered to mud and clay. The stratigraphy exposed in the Rio Desague fault scarp is comprised of approximately equal volumes of lava flows and pyroclastic material. On the other hand, younger stratigraphy exposed in the Main Crater consists of three to four times more pyroclastic material than lava flows. The high ratio of pyroclastics to lavas in the Main Crater stratigraphy is consistent with historic eruptive

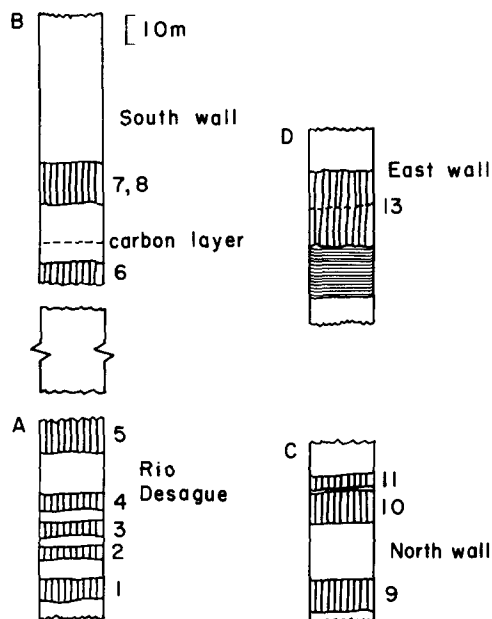


Fig. 3. Stratigraphic sections from the summit region. Sections A–D show the stratigraphic position of 12 of the 14 stratigraphically ordered summit samples. Sample #12, not shown, is best exposed on the western wall of the Main Crater and #14 is the 1954 lava from the floor of the crater. The Rio Desague section is 1 km west of the center of the Main Crater and just below Cerro Pelon. A section of unknown thickness is missing between A and B. Lava shown as vertical lined pattern, lake sediments as horizontal lined pattern, tephra is clear.

activity, which is dominantly explosive.

A stratigraphic section, exposed by the Rio Desague fault scarp, begins with a thick tephra unit of unknown character, possibly the Lapilli Tuff. There was no safe access to outcrops of this tephra. Above the tephra are flat-lying lava flows interbedded with air fall tephra (#1–5 in Fig. 3a). The azimuths of elongate vesicles in the lava indicate that the source vent was Botos Cone. The flat-lying attitudes suggest that caldera walls restricted the lavas to the summit. Therefore, eruptions from Botos Cone served primarily to fill the existing inner caldera.

Eruptions from Botos Cone also post-date movement along the Rio Desague fault. In a section exposed in the southern wall of the Main Crater, there are lava flows from Botos Cone

that mantle the fault scarp (#6–8 in Fig. 3b). A four-inch diameter carbonized tree branch found in tephra between those scarp mantling flows yielded a radiocarbon age of $7,540 \pm 100$ years (U.S.G.S. Sample #W5229; Prosser, 1983). Cessation of Botos Cone volcanism followed soon after deposition of the carbon-bearing tephra.

The stratigraphy associated with eruptions from the Main Crater is well exposed in the near-vertical walls of the Main Crater. Thick deposits of poorly sorted tephra are interlayered with lava flows. The tephra are characterized by a chaotic mixture of unsorted lapilli, bombs, blocks and ashy matrix. Individual tephra units may exhibit bedding and normal sorting, and range in thickness from 0.5 to 15 m. These pyroclastic units are remarkably uniform in appearance and indicate a consistent eruptive style consisting of small to moderate sized phreatic, phreatomagmatic, and vulcanian eruptions. This is also the present pattern of activity at Poás. A distinctive red pyroclastic unit of well-sorted, bedded, vesiculated, juvenile lapilli (#12, Table 1) crops out at the top of the southwest rim of the crater. The stratigraphic position and unique character of this deposit suggests that it was erupted just prior to collapse of the Main Crater, and may in fact be the result of the crater-forming eruption. This unit reaches five meters in thickness in the western wall of the Main Crater.

Three lava flows, erupted before the collapse of the Main Crater, are exposed in the northern and northwestern walls (#9–11 in Fig. 3c). Older flows from Botos Cone created physical barriers preventing flow to the west and east and the Rio Desague fault scarp blocked flow to the south. Each of these flows exhibit well-developed sheet and cooling joints, as well as rubbly flow tops and bottoms. The middle and upper flows are separated by less than a meter of rubble or tephra. Mudflows, exposed within the western flank graben adjacent to the Main Crater, were also deposited prior to the collapse of the Main Crater.

TABLE 1

Major- and trace-element analyses of Poás samples

Sample: Group: #:	P08393 S 1	P08394 S 2	P08395 S 3	P08396 S 4	P08397 S 5	P08310 S 6	P08340 Ti 7	P08317 Ti 8	P0839 S 9
SiO ₂	57.55	57.98	54.88	56.18	51.47	50.48	52.52	49.10	64.57
TiO ₂	0.72	0.70	0.73	0.74	0.83	0.77	1.03	1.05	0.50
Al ₂ O ₃	16.79	16.44	16.71	16.80	18.32	17.41	16.89	15.52	15.80
FeO	7.72	7.12	7.61	8.03	10.09	10.05	9.80	9.47	4.64
MnO	0.14	0.13	0.15	0.16	0.18	0.18	0.18	0.15	0.10
MgO	3.35	3.21	3.47	3.63	5.59	5.01	4.44	7.11	1.67
CaO	6.94	6.63	6.61	7.13	10.23	9.98	9.03	9.44	4.38
Na ₂ O	3.28	3.22	2.91	3.15	2.56	2.25	2.81	2.46	3.37
K ₂ O	1.66	1.75	1.44	1.55	0.86	0.85	1.46	1.52	2.57
P ₂ O ₅	0.17	0.18	0.16	0.19	0.16	0.14	0.27	0.42	0.16
H ₂ O	<u>0.88</u>	<u>1.03</u>	<u>2.12</u>	<u>1.04</u>	<u>0.43</u>	<u>2.19</u>	<u>1.30</u>	<u>2.05</u>	<u>1.53</u>
Total	99.20	98.39	96.79	98.56	100.70	99.31	99.73	98.29	99.29
Rb	37	26	13	24	26	8	31	33	71
Ba	767	829	728	768	439	487	619	708	976
Sr	474	490	471	519	553	577	622	738	428
V	190	199	192	227	292	287	326	240	90
Cr	32	32	33	45	37	51	27	221	33
Ni	12	15	10	21	21	22	16	112	10
Zr	118	145	114	133	80	97	102	146	177
Sc	23	23	23	26	31	32	34	28	11
Cu	67	98	83	91	113	160	118	51	79

Sample: Group: #:	P08369 S 10	P0838 S 11	P08312 S 12	P0835 S 13	P08398 S 14	P08319 Al	P08349 Al	P02 Al	P03 Al
SiO ₂	57.13	53.98	61.54	57.14	54.63	59.55	54.47	51.13	62.15
TiO ₂	0.62	0.75	0.58	0.69	0.80	0.69	0.84	0.75	0.62
Al ₂ O ₃	16.75	17.39	16.37	17.50	18.18	18.29	18.89	19.64	18.78
FeO	7.40	9.21	5.60	7.71	8.70	5.60	6.97	8.99	3.77
MnO	0.16	0.14	0.13	0.14	0.15	0.12	0.13	0.18	0.10
MgO	3.13	4.20	2.38	3.42	4.78	2.25	2.69	5.55	1.17
CaO	7.36	7.99	5.35	7.53	9.21	6.61	7.51	9.61	5.96
Na ₂ O	3.04	2.75	2.94	2.92	2.99	3.39	3.21	2.89	4.05
K ₂ O	1.62	1.20	2.00	1.65	1.04	2.11	1.43	0.75	2.51
P ₂ O ₅	0.16	0.17	0.18	0.17	0.13	0.22	0.24	0.16	0.23
H ₂ O	<u>0.98</u>	<u>1.08</u>	<u>2.10</u>	<u>1.23</u>	<u>0.38</u>	<u>0.62</u>	<u>2.21</u>	<u>0.30</u>	<u>0.26</u>
Total	98.35	98.84	99.17	99.65	100.99	99.45	98.69	99.95	99.60
Rb	37	18	61	50	27	64	40	10	72
Ba	685	561	814	698	468	794	628	377	1059
Sr	566	598	525	542	565	525	584	622	595
V	179	246	116	213	269	142	220	272	73
Cr	27	34	7	28	27	12	25	48	8
Ni	12	13	9	15	14	3	30	31	2
Zr	129	119	126	149	94	150	111	75	199
Sc	19	24	13	23	28	16	23	28	13
Cu	111	110	56	100	121	67	102	92	31

TABLE 1 (continued)

Sample: Group:	P04 Al	P01 Al	P06 Ti	P07 Ti	P08 Ti	P09 Ti	P010 Ti	P08363 LT	P08387 LT
SiO ₂	54.21	54.07	58.43	55.66	58.73	56.59	52.36	54.30	52.14
TiO ₂	0.79	0.99	0.90	1.06	0.92	1.04	1.11	1.00	0.97
Al ₂ O ₃	19.35	19.81	16.85	16.76	17.04	16.85	18.24	17.09	17.93
FeO	7.71	7.49	7.17	8.87	7.43	8.85	9.92	9.18	9.38
MnO	0.16	0.14	0.16	0.17	0.17	0.17	0.19	0.17	0.16
MgO	3.84	2.66	2.80	3.68	2.98	3.11	3.89	3.82	4.38
CaO	8.61	8.14	6.38	7.80	6.74	6.95	8.25	8.15	8.78
Na ₂ O	3.09	3.62	3.64	3.31	3.64	3.09	3.16	2.76	2.66
K ₂ O	1.06	1.97	2.12	2.03	2.07	2.01	1.24	1.45	1.04
P ₂ O ₅	0.20	0.40	0.26	0.31	0.26	0.28	0.27	0.22	0.19
H ₂ O	<u>0.24</u>	<u>0.21</u>	<u>0.46</u>	<u>0.20</u>	<u>0.16</u>	<u>0.56</u>	<u>0.45</u>	<u>1.37</u>	<u>1.65</u>
Total	99.26	99.50	99.17	99.85	100.14	99.50	99.08	99.51	99.29
Rb	21	44	64	59	62	59	24	44	31
Ba	630	956	788	816	782	793	768	610	520
Sr	690	841	507	573	515	520	583	536	588
V	231	230	180	291	193	309	331	281	275
Cr	17	20	13	13	6	11	30	12	23
Ni	10	13	3	8	2	9	12	14	15
Zr	96	180	159	167	161	165	157	136	115
Sc	24	25	24	31	25	31	35	30	32
Cu	149	277	106	150	110	287	158	155	146

is the order in the stratigraphically collected sequence from the summit; 1 is lowest, 14 is from the 1953-1955 eruption. Groups: S for summit, Ti for TiO₂-rich, Al for Al₂O₃-rich, Lt for Lapilli Tuff.

Deposits produced after the collapse of the Main Crater are primarily pyroclastic, but include two lava flows and lacustrine volcanoclastic sediments. In addition, two further collapses have occurred within the Main Crater. At the base of the stratigraphic section formed after the initial collapse is a thick, chaotic, unsorted tephra, which is overlain by well-bedded lacustrine sediments and lake-deposited ash and tephra. The lakebeds are best exhibited in the eastern portion of the crater and show soft sediment deformation structures and bomb sags. The beds in many cases are thin and continuous. The lake sediments are altered to clay and alunite and include fine-grained disseminated sulfur, as well as thin crosscutting sulfur veins. The lacustrine sediments represent a quiescent period in the volcano's history, punctuated by infrequent, mildly explosive eruptions. The quiescent period appears to have occurred just after the initial crater collapse.

The very well-developed thin bedding and fine-grained texture of the lacustrine sediments may be an indication of varve-like deposition of these sediments. More than fifty individual beds can be distinguished in the uppermost lake sediments, possibly indicating a fifty-year hiatus between eruptions.

The initial collapse of the Main Crater exposed native sulfur veins up to 40 cm thick in the north wall of the crater, approximately two-thirds of the way from the floor to the rim. These sulfur veins are similar to, but larger than, the sulfur veins in the lacustrine sediments just described. The sulfur veins in the crater wall represent feeder pipes for an earlier generation of fumaroles prior to the initial crater collapse. Active fumaroles beneath the present crater lake are in the process of forming more such sulfur veins. When the lake level is low, sulfur tubes on the shores of the lake project up to 20 cm above the thixotropic lake bottom sedi-

ments. It would seem that during past eruptive hiatuses Poás degassed in a manner very similar to that seen today.

Overlying and deforming the lake sediments and volcanoclastics is a 30-m-thick andesitic lava flow (#13 in Fig. 3d). The geometry of cooling and sheet joints and the presence of rubbly sections in the central portion of this flow indicate that the flow ramped over itself as it became restricted by the walls of the crater. Shortly after extrusion of this flow, a second crater collapse, approximately one third the volume of the initial crater gave the Main Crater its present dimensions. The development of an intra-crater cinder cone, lava flow, and pit crater were the result of the 1953–1955 eruptive activity described earlier (#14, Table 1). Unsorted, blocky to ashy pyroclastic deposits from small phreatic eruptions both pre-date and post-date deposits from the 1953–1955 activity.

On the basis of the summit stratigraphy just described, the development of the summit since the formation of the inner caldera proceeded as follows. First, eruptions produced the Von Frantzius Cone and then Botos Cone became the active vent. Initially, Botos Cone produced nearly equal volumes of pyroclastic materials and lava flows, both of which helped fill in the existing caldera. Toward the end of activity at Botos Cone the west flank of the volcano subsided, exposing the caldera-filling volcanics. Activity at Botos Cone resumed, and several flows mantled the newly formed Rio Desague fault scarp. At this point eruptive activity shifted to the Main Crater where a thick pile, consisting primarily of pyroclastic material, was built up over time. Following eruption of a distinctive red pyroclastic unit, composed primarily of juvenile lapilli, the initial collapse of the Main Crater occurred. A lake formed in the crater and activity was restricted to small explosive eruptions with intervening periods of quiescence in which finely bedded lacustrine sediments were deposited. Extrusion of an intra-crater lava flow that deformed the lacustrine sediments, and another crater collapse gave the

Main Crater its present morphology. Activity from this time to the present has consisted of small explosive eruptions and periods of quiescence. The intra-crater cone and the small pit crater, site of the present crater lake, were formed during the 1953–1955 eruptive activity.

Sample locations and geochemical data

Major- and trace-element data on 27 samples from Poás are given in Table 1. Analyses were by DCP-AES (Feigenson and Carr, 1985). The stratigraphy of fourteen recent samples is outlined above and in Fig. 3. The stratigraphic order of these samples is given in Table 1 and Fig. 3. Thirteen other samples without precise stratigraphic control were also analysed in order to roughly categorize the earlier lavas from Poás. The Lapilli Tuff is represented by P08363 and P08387. The Von Frantzius cone is represented by P08349, collected just north of the active crater. P08319 is a sample of Botos Cone with an indeterminate stratigraphic position. The other 9 samples (P01 to P010) are from widely scattered sites on the flanks of Poás with sample locations given in Fig. 2.

Petrography

Basalts from the summit region and the flanks are not petrographically distinguishable. All are porphyritic with an intergranular to intersertal groundmass. Plagioclase is the dominant phenocryst with 20–40 modal % (Prosser, 1983). Magnetite and augite are present in each basalt. Orthopyroxene is present in some basalts and olivine and orthopyroxene are present in P02.

Andesites collected at the summit and along the northeast flank are two pyroxene andesites with abundant plagioclase and magnetite phenocrysts as well. All have porphyritic-pilotaxitic textures and most have glomeroporphyritic clusters of the phenocryst phases. Olivine is rarely present in these clusters and always mantled by pyroxene. Traces of pale brown,

weakly pleochroic hornblendes are present in P03, the sample with the highest Na_2O content.

Andesites, collected on the south flank near Sabana Redonda and from one site on the north flank, are distinctively aphyric or nearly aphyric. The rare microphenocrysts are plagioclase, magnetite and augite. Olivine is extremely rare and pigeonite rims are present in the most siliceous samples, P06 and P08. P01 is a mixture of basaltic lava with abundant large plagioclase phenocrysts (up to 5 mm long) and an andesite lava with a pilotaxitic texture. Since the bulk analysis of a mixture is not particularly meaningful, this sample is not included in the discussion of petrology and geochemistry.

Results

Definition of groups

The 14 stratigraphically constrained samples from the summit region can be divided into two geochemically distinct groups. The main group consists of three felsic to mafic sequences #1–#6, #9–#11 and #12–#14. The lavas of these three sequences are essentially colinear in any variation diagram and they comprise the summit group which includes and represents the most recent activity of Poás (#14 is from the 1953 eruption). Two samples, #7 and #8, are geochemically distinct, most notably in TiO_2 and P_2O_5 . These are part of the Ti-rich group defined below.

Most of the remaining samples can be divided into two groups (Fig. 4), an Al-rich group ($\geq 18.25\% \text{Al}_2\text{O}_3$) that erupted primarily from vents north of the Main Crater and a Ti-rich group with $> 0.9\% \text{TiO}_2$. The Al-rich group includes samples from the young intra-caldera cone at Laguna Hule (P02) the Von Frantzius Cone (P08349, P03, P04), and Botos Cone (P08319). Sample P08319 was collected at Botos Cone from an indeterminate stratigraphic position. Except for this sample, all the Al-rich samples erupted from vents north of the Main Crater. They cover a wide range of ages,

so they have a geochemical and spatial identity but not a temporal one. Given the large area and long time interval spanned, this group should be considered conditional. Further mapping will undoubtedly show that it can be divided into several units.

The Ti-rich group includes P08340 and P08317, #7 and #8 in the summit stratigraphy, P06 collected from the east flank of Poás in the lower drainage of Botos Cone, and samples from the area of the Sabana Redonda cinder cones (P07, P08, P09, P010). The Ti-rich group has distinct geochemistry and distinct location (Botos Cone or south flank). Summit mapping indicates that this group also had a limited time duration.

The remaining samples, P08363 and P08387, are from the Poás Lapilli Tuff. Geochemically, these samples do not fit with either of the three groups described above. For most elements they are similar to the summit group, but they have slightly higher TiO_2 .

Compositional variations

Samples from the summit group (filled squares) define narrow linear trends in the variation diagrams (Figs. 4–6). The three felsic to mafic sequences are colinear and therefore not given separate symbols. The geochemical variation of this group is typical of the normal, calc-alkaline fractionation style found at most other Central American volcanoes (Carr et al., 1982). Mineral analyses are not presently available for Poás and so the precise fractionation model responsible for the well-defined summit trend cannot be exactly specified. However, an approximate model can be outlined using the least-squares technique of Bryan et al. (1968) and appropriate mineral analyses from similar Central American volcanoes. Within the error of analysis the summit andesites from Poás are derived from the basalts by about 45% crystallization (Table 2A).

The Al-rich samples (crosses) have geochemical variations similar to those of the sum-

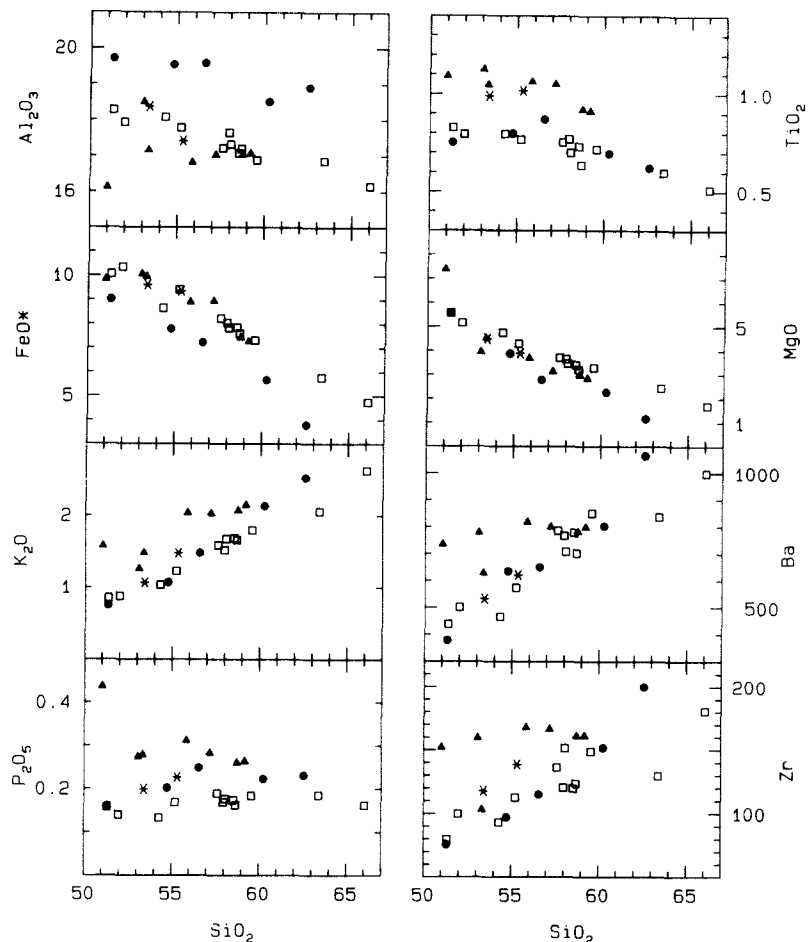


Fig. 4. Harker variation diagram. Circles are Al-rich group. Triangles are Ti-rich group. Squares are summit group. Asterisks are Poás Lapilli Tuff. Samples recalculated to 100% on a water-free basis prior to plotting.

mit group but displaced to higher Al_2O_3 , Sr, Na_2O and P_2O_5 and lower FeO and MgO. Since the Al-rich group was collected from several vents and over a wide span of ages, there is no suggestion that these samples should be related by a particular fractionation model. They probably all evolved separately from similar parental magma and under similar conditions.

The Ti-rich group (triangles) is unusual for several reasons. First, the silica-rich members of this group are distinctly aphyric. Second, the variations with increasing SiO_2 of Al_2O_3 and several incompatible elements show considerable scatter, implying that there is no simple liquid line of descent relating these nearly

aphyric lavas. Third, for the andesites Zr, Ba and K do not increase with SiO_2 but stay the same or decrease. This is further evidence that this group of lavas cannot be related by simple fractional crystallization of the observed phenocrysts. Finally, the uniformly thin soil cover and small degree of weathering suggest that the Ti-rich lavas in the Sabana Redonda area were erupted over a brief span of time in the recent past. The two Ti-rich samples in the summit stratigraphy appear to be the last lavas erupted from Botos Cone. The aphyric flank lava flows in the Sabana Redonda area erupted above the Lapilli Tuff, which makes them the youngest lavas on the flanks of Poás and suggests corre-

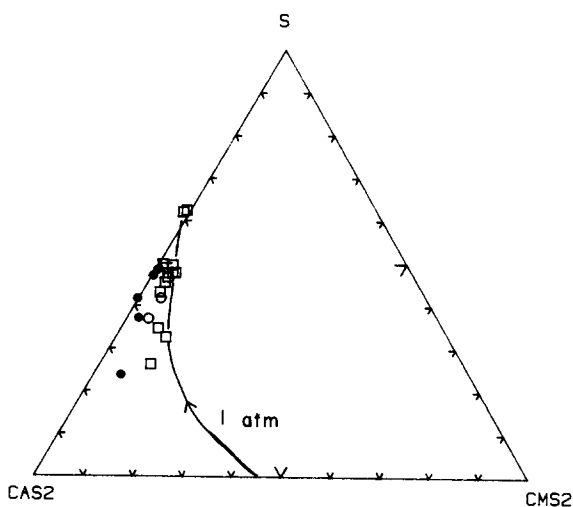
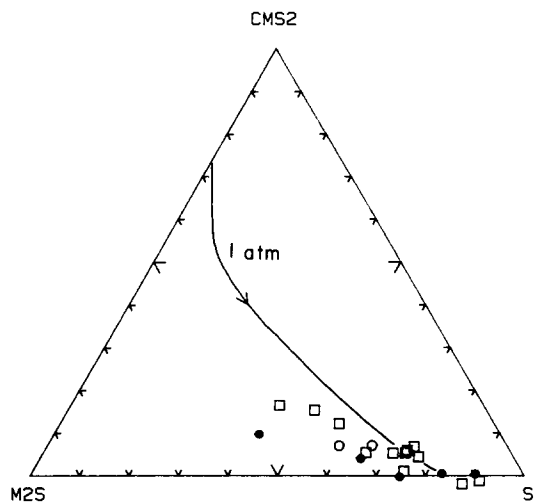


Fig. 5. Pseudo-ternary phase diagrams projected from olivine (bottom) and plagioclase (top). Open circles are Lapilli Tuff. Other symbols as in Fig. 4. 1 atm cotectic from data of Walker et al. (1979). Projection after Carr (1984).

lation with the geochemically similar lavas at the summit. The radiocarbon age of about 7500 yr. B.P. for tephra covered by the last flow from Botos Cone is consistent with the low degree of weathering of the aphyric flank flows in the Sabana Redonda area.

The Ti-rich group appears to represent a brief eruptive episode, that accompanied a significant structural modification of the volcano and led to an atypical flank eruption. The apparent structural-stratigraphic brevity of this episode

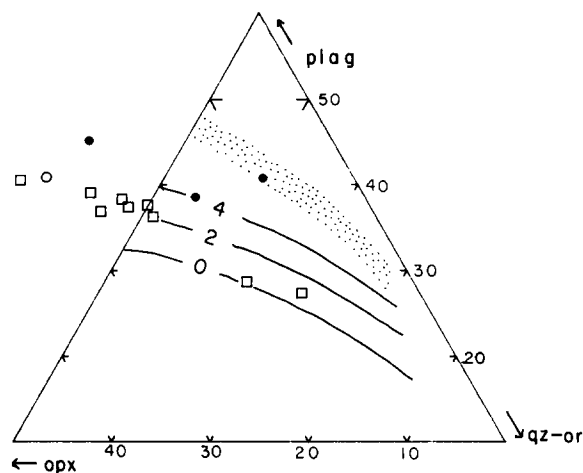


Fig. 6. Pseudo-ternary phase diagram projected from diopside using the method of Merzbacher and Eggler (1984) and including their contours of wt.% H₂O. Stipple marks stability field of amphibole. Symbols as in Fig. 5.

and the petrographic similarity of the lavas is not matched by geochemical consistency.

We do not have an adequate model for the origin of the Ti-rich group of lavas, but the aphyric character of the andesites suggests that they were superheated, possibly as a result of magma mixing (Walker et al., 1979; Gerlach and Grove, 1982). Magma mixing is further suggested by the variation in incompatible elements with SiO₂. P08317, the most magnesium-rich member of this group is a phyric basalt. Removal of calcic plagioclase and olivine or orthopyroxene from this sample followed by mixing with various members of the summit group can approximately yield the intermediate to high silica members of the Ti-rich group (see example in Table 2B). None of the Ti-rich samples can be produced by simple mixing of the P08317 basalt and any member of the summit group, some removal of plagioclase and a Mg-rich mineral is always needed; and even then, the fit is not that convincing (Table 2B).

In pseudoternary CMAS projections from early crystallizing minerals (Fig. 5) the summit group and the Al-rich group define narrow trends that parallel the experimentally determined 1 atm cotectics of Walker et al. (1979),

TABLE 2

Fractionation and mixing models for Poás

A. The Parent lava, P08397, is made from:

Model %	Cumulate %	
4.4	9.3	Mt
27.6	58.0	P1 An 75
9.8	20.5	Cpx Wo44-En47
5.9	12.3	O1 Fo 72
52.3	-	daughter (P08393)

P08397	SiO ₂	TiO ₂	Al ₂ O ₃	FeO	MnO	MgO	CaO	Na ₂ O	K ₂ O	P ₂ O ₅
Observed	51.33	0.83	18.27	10.06	0.17	5.57	10.20	2.55	0.85	0.16
Calculated	51.32	0.86	18.29	10.06	0.13	5.57	10.20	2.52	0.91	0.09
Residual	0.00	-0.03	-0.01	0.00	0.05	-0.00	0.00	0.04	-0.06	0.07

Sum of squares of weighted residuals = 0.01

B. The Hybrid lava, P08340, is made from:

%		
7.0	P1 An75	(removed)
5.5	O1 Fo78	(removed)
64.4	P08317	(mixed)
48.1	P0838	(mixed)

P08340	SiO ₂	TiO ₂	Al ₂ O ₃	FeO	MnO	MgO	CaO	Na ₂ O	K ₂ O	P ₂ O ₅
Observed	53.36	1.05	17.16	9.96	0.18	4.51	9.17	2.85	1.48	0.28
Calculated	53.86	1.07	16.74	0.66	0.15	4.59	9.15	2.81	1.60	0.36
Residual	-0.20	0.02	0.21	0.30	0.03	-0.08	0.02	0.05	-0.12	0.08

Sum of squares of weighted residuals = 0.203

but appear to define shrunken primary phase volumes for olivine and plagioclase. The Ti-rich group, which may be a mixture, is not considered. Data from other Central American volcanoes show shrinkages of the olivine and plagioclase fields that are proportional to crustal thickness (Carr, 1984). The data from Poás suggest two different magma chambers feeding the volcano, a deeper or more water-rich one supplying Al-rich magma to the northern side of the volcano and a slightly less deep or less water-rich one supplying Botos Cone and the

Main Crater. Experimental data are inadequate to specify depths, but the Al-rich group may originate near the Moho (about 40 km here) and the summit group may originate within the lower or middle crust. Similarly deep magma chambers have been proposed for Costa Rican volcanoes by Kussmaul et al., 1982 and Thorpe and Francis (1981). The experimental data of Baker and Egger (1983) suggest that the Al-rich group evolved from basalts with a water content 1-2% and that the summit group evolved from basalts with a lower water content.

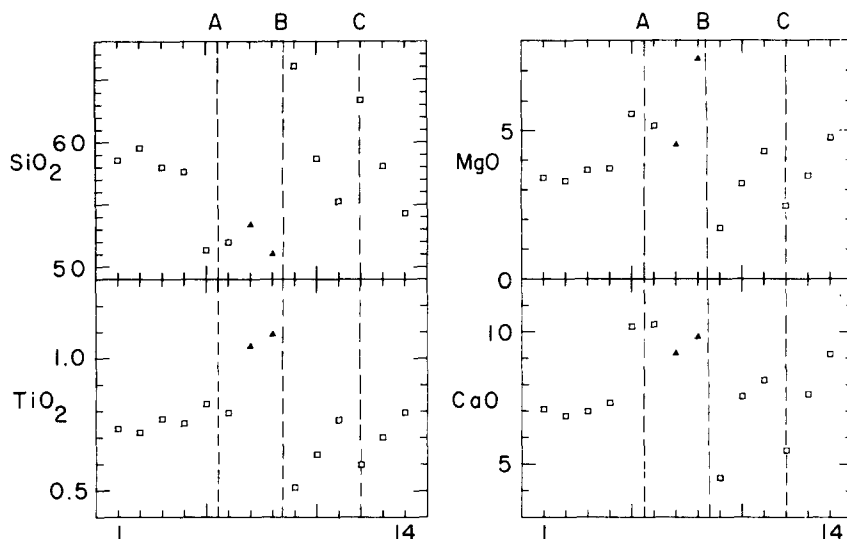


Fig. 7. Stratigraphic variation in selected major oxides. 1 is earliest and 14 is latest. Symbols as in Fig. 4. A, B, C mark times of major structural changes. A is movement along the Rio Desague fault scarp and opening of the west flank graben. B is movement of the active vent from Botos Cone to the site of the present Main Crater. C is the major collapse forming the Main Crater.

For andesites and dacites subject to pressures less than 0.5 Gpa and $p_{\text{H}_2\text{O}} < p_{\text{total}}$, Merzbacher and Eggler (1984) have calibrated a geohygro-meter. Liquid compositions in equilibrium with plagioclase, orthopyroxene and clinopyroxene vary with water content more than they vary with pressure. Using the projection of Merzbacher and Eggler (1984) the silicic extrusives of the summit group and the most silicic sample of the Poás Lapilli Tuff appear to have evolved along the 3% H_2O contour. The two most silicic samples may have had less than 2% H_2O prior to eruption. Lavas of the Al-rich group, which erupted primarily from the northern vents, appear to have evolved at higher H_2O contents, approximately comparable to those deduced for Mt. St. Helens by Merzbacher and Eggler (1984). One sample, P03, plots in the field of amphibole crystallization and has amphibole microphenocrysts.

Water content is an important factor controlling explosivity and volcanic hazard. The available data from Poás suggest that the vents for the Al-rich group, primarily Von Frantzius and Cerro Congo, have a greater potential for

violently explosive eruptions. However, the presence of extensive deposits of Poás Lapilli Tuff demonstrate that the slightly lower inferred H_2O contents for the summit group are still sufficient to generate a large tephra eruption.

Temporal variation

Figure 7 depicts major oxide and minor element variation of the 14 summit samples with respect to their stratigraphic position. Although the samples are equally spaced in the diagram, it should be pointed out that the time interval between each sample is not constant. In particular, there is a long time interval between #5 and #6, during which there was over 300 meters of vertical movement along the Rio Desague fault.

The three felsic to mafic sequences mentioned above can be seen in Fig. 7. In a similar study of temporal chemical variation, Newhall (1979) refers to compositional changes over the span of several eruptions as medium-term variation. The limited number of samples here per-

mits examination of medium-term temporal magmatic variation, but does not allow us to define the total long-term evolution of the volcano. The time span covered by each sequence is believed to be on the order of three to ten thousand years.

The felsic to mafic compositional sequences found at Poás add to the variety of temporal variations found at Central American volcanoes. Several volcanoes experienced mafic to felsic temporal magmatic variations, (Santa Mariá, Rose et al., 1977; Boqueron, Fairbrothers et al., 1978; Izalco, Woodruff et al., 1979). Izalco volcano (Carr and Pontier, 1981) has experienced a crude felsic to mafic temporal variation, which, in detail, is related to progressively shorter repose intervals. The summit crater of Santa Ana volcano exposes a short sequence of lavas that may represent an inverted magma chamber, with a graded silicic top and a uniform mafic bottom (Carr and Pontier, 1981). Upon eruption this stratigraphy was inverted giving a short term felsic to mafic trend.

The felsic to mafic trends in Fig. 7 can be explained in terms of repeated similar fractionation of a common parent magma. Initial eruptions in each sequence derive magma from the uppermost portion of the magma chamber which has been compositionally zoned by crystal fractionation and fluid mechanical processes in the magma chamber (McBirney et al., 1985). As the sequence progresses, magma is derived from deeper within the chamber causing eruption of more mafic, less fractionated lavas. The long duration interpreted for these sequences suggests a large, slowly cooling magma chamber deep within the crust. Thorpe and Francis (1981), proposed a magma chamber for Poás at lower crustal levels on the basis of gravity measurements.

The transitions between the three felsic to mafic sequences occur at significant points in the evolution of the summit. All of the lavas of sequence 1 (#1–6, Table 1) were erupted from Botos Cone and all the lavas of sequence 2

(#9–11) were erupted from the Main Crater. Therefore, the transition was marked by a change in the location of the active vent and emission of the high TiO_2 lavas (#7 and #8). The Main Crater attained its present dimensions during a large collapse following the eruption of tephra from which sample #12 was collected. This eruption marks the beginning of sequence 3. Thus, this transition also coincided with a major change in the active summit vent, possibly as a result of arrival of new magma at the summit or a hiatus during which fractionation of existing magma could have taken place. The chemical composition of the 1953–1955 lava indicates that the present sequence has reached basaltic andesite composition which may represent the end of the sequence.

Discussion

Cycles of recent activity

The field mapping and stratigraphically ordered compositional variations allow a simple model of the most recent history of the volcano. Major changes in the chemical composition of lavas accompany major geological events at the summit. Two observations stand out; first, lavas with high silica contents have signalled the beginning of a new magma sequence and changes in location or structure of the active vent. Second, when lava compositions become mafic (50–55% SiO_2), the end of an eruptive sequence is near. Because the lavas comprise only 20–50% of the stratigraphy and highly altered pyroclastics comprise the rest, we emphasize that these observations are a model, not a comprehensive description.

The magmatic sequences in Fig. 7 define crudely cyclical behavior for the activity at Poás. The largest recent explosive eruption, #12, and the flank-related activity, #7 and #8, both occurred at transitions between cycles. Unfortunately, the stratigraphic axis in Fig. 7 is relative, not absolute time. Furthermore, there are gaps in the record since most pyroclastic depos-

its were highly altered and therefore not sampled. Although, the first sequence appears quite different, this could simply result from differences in exposure, in distance from the active vent and in preservation.

Absolute dating of the flows and scoria that comprise the summit stratigraphy is needed to verify the apparently cyclic nature of the magmatic sequences. Most importantly, absolute dating would answer the major question about present volcanic hazard: does the mafic character of recent eruptions insure a long pause before crystal fractionation can produce another batch of explosive silicic magma; or, do batches of fractionated magma rise from deep in the crust, dislodge or bypass the remaining mafic magma from the previous sequence and initiate the explosive phase of a new cycle without pause?

Acknowledgements

We are indebted to R.E. Stoiber and S.N. Williams for their assistance in the course of this study and preparation of this paper. Eduardo Malavassi and the members of the Volcanology Program at the Universidad Nacional in Heredia, Costa Rica gave valuable field assistance. Thanks also to Meyer Rubin, U.S.G.S. Radiocarbon Laboratory, for radiocarbon age determination. M.D. Feigenson and J.A. Walker suggested several improvements in the manuscript. This research was funded by grants from Sigma Xi, The Explorers Club, the Department of Earth Sciences of Dartmouth College, and the National Science Foundation, grant EAR-8007424 and grant EAR-8318668.

References

- Allègre, C.J. and Condomines, M., 1976. Fine chronology of volcanic processing using ^{238}U - ^{230}Th systematics. *Earth Planet. Sci. Lett.*, 28: 395-406.
- Baker, D.R. and Egger, D.H., 1983. Fractionation paths of Atka (Aleutians) high alumina basalts: constraints from phase relations. *J. Volcanol. Geotherm. Res.*, 18: 387-404.
- Bennett, F.D. and Raccichini, S.M., 1978. Subaqueous sulfur lake in Volcan Poás. *Nature*, 271: 342-344.
- Bryan, W.B., Finger, L.W. and Chayes, F., 1969. Estimating proportions in petrographic mixing equations by least-squares approximation. *Science*, 163: 926-927.
- Carr, M.J., 1984. Symmetrical and segmented variation of physical and geochemical characteristics of the Central American volcanic front. *J. Volcanol. Geotherm. Res.*, 20: 231-252.
- Carr, M.J. and Pontier, N.K., 1981. Evolution of a young parasitic cone towards a mature vent; Izalco and Santa Ana volcanoes in El Salvador, Central America. *J. Volcanol. Geotherm. Res.*, 11: 277-292.
- Carr, M.J., Rose, W.I., Jr and Stoiber, R.E., 1982. Central America. In: R.S. Thorpe (Editor), *Orogenic Andesites*. John Wiley, New York, NY, pp. 149-166.
- Casertano, L., Borgia, A. and Cigolini, C., 1983. El Volcan Poás, Costa Rica: Cronología y características de actividad. *Geofis. Int.*, 22(3): 215-236.
- Fairbrothers, G.E., Carr, M.J. and Mayfield, D.G., 1978. Temporal magmatic variation at Boqueron Volcano, El Salvador. *Contrib. Mineral. Petrol.*, 67: 1-9.
- Feigenson, M. and Carr, M.J., 1985. Determination of major, trace and rare earth elements in rocks by DCP-AES. *Chem. Geol.*, 51: 19-27.
- Francis, P.W., Thorpe, R.S. and Brown, C.G., 1980. Pyroclastic sulfur eruption at Poás Volcano, Costa Rica. *Nature*, 283: 754-756.
- Gerlach, D.C. and Grove, T.L., 1982. Petrology of Medicine Lake Highland volcanics: Characterization of the end members of magma mixing. *Contrib. Mineral. Petrol.*, 80: 147-159.
- Kussmaul, S., Paniagua, S. and Gainsa, J., 1982. Recopilación, clasificación e interpretación petroquímica de los rocas de Costa Rica. Informe Semestral Inst. Geog. Nac. Jul.-Dec. 1982, San Jose, Costa Rica, pp. 17-79.
- Krushensky, R.D. and Esvalante, G., 1967. Activity of Irazú and Poás volcanoes, Costa Rica, November 1964-July 1965. *Bull. Volcanol.*, 31: 75-84.
- McBirney, A.R., Baker, B.H. and Nilson, R.H., 1985. Liquid fractionation. Part I: basic principles and experimental simulations. *J. Volcanol. Geotherm. Res.*, 24: 1-24.
- Merzbacher, C. and Egger, D.H., 1984. A magmatic geohygrometer: Application to Mount St. Helens and other dacitic magmas. *Geology*, 12: 587-590.
- Molnar, P. and Sykes, L.R., 1969. Tectonics of the Middle America regions from focal mechanisms and seismicity. *Geol. Soc. Am. Bull.*, 80: 1639-1684.
- Nakamura, K., 1977. Volcanoes as possible indicators of tectonic stress orientation - principle and proposal. *J. Volcanol. Geotherm. Res.*, 2: 1-16.
- Newhall, C.G., 1979. Temporal variation in the lavas of Mayon Volcano, Philippines. *J. Volcanol. Geotherm. Res.*, 6: 61-83.

- Prosser, J.T., 1983. The geology of Poás volcano, Costa Rica. Ms. Thesis, Dartmouth College, Hanover, NH, 165 pp. (unpubl.).
- Prosser, J.T., 1986. Geology and medium-term temporal variation found at the summit region of Poás volcano, Costa Rica. *Bol. Vulcanol. Heredia, Costa Rica*, 15: 21-39.
- Rose, W.I., Grant, N.K., Hahn, G.A., Lange, I.M., Powell, J.L., Easter, J. and Degraff, J.M., 1977. The evolution of Santa Mariá Volcano, Guatemala. *J. Geol.*, 85: 63-87.
- Rymer, H. and Brown, G.C., 1984. Periodic gravity changes at Poás Volcano, Costa Rica. *Nature*, 311: 243-245.
- Sáenz, R., 1982. Edades radiométricas de algunas rocas de Costa Rica. *Bol. Vulcanol., Heredia, Costa Rica*, 12: 8-10.
- Simkin, T., Siebert, L., McClelland, L., Bridge, D., Newell, C. and Latter, J.H., 1981. *Volcanoes of the World*. Hutchinson Ross, Stroudsburg, PA, 232 pp.
- Stoiber, R.E. and Carr, M.J., 1973. Quaternary volcanic and tectonic segmentation of Central America. *Bull. Vulcanol.*, 37: 326-337.
- Thorpe, R.S. and Francis, P.W., 1981. Magma chamber below Poás Volcano, Costa Rica. *J. Geol. Soc. London*, 138: 367-373.
- Vargas, C.A. (editor), 1979. *Antología: El Volcan Poás*. San Jose, 120 pp.
- Walker, D., Shibata, T. and DeLong, S.E., 1979. Abyssal tholeiites from the Oceanographer fracture zone, II-phase equilibria and mixing. *Contrib. Mineral. Petrol.*, 70: 111-125.
- Williams, H., 1952. Volcanic history of the Meseta Central Occidental, Costa Rica. *Univ. Calif. Publ., Geol. Sci.*, 29: 145-180.
- Woodruff, L.G., Rose, W.I. and Rigot, W., 1979. Contrasting fractionation patterns for sequential magmas from two calc-alkaline volcanoes in Central America. *J. Vulcanol. Geotherm. Res.*, 6: 217-240.